

Laser-Induced Breakdown Spectroscopy for Ambient Air Particulate Monitoring: Correlation of Total and Speciated Aerosol Particle Counts

B. HETTINGER, V. HOHREITER, M. SWINGLE, and D. W. HAHN*

Department of Mechanical and Aerospace Engineering, University of Florida, Gainesville, Florida 32611-6300

A statistical analysis of ambient air particle monitoring, namely PM_{2.5}, is presented to elucidate the correlations between laser-induced breakdown spectroscopy (LIBS)-based speciated aerosol monitoring and non-speciated aerosol monitoring (i.e., total particle counts). LIBS was used in a real-time, conditional-processing mode to identify individual aerosol particles containing detectable quantities of either calcium or sodium, as based on the resulting atomic emission signals. Using this technique, real-time measurements of speciated aerosol particle concentrations and analyte mass concentrations were evaluated for a total of 60 1-hour sampling periods spread over a 5-week period. For each 1-hour sampling period, total aerosol counts were simultaneously monitored using a commercial light scattering-based instrument. Over the 30 sampling periods, aerosol counts (both total and LIBS-based) were found to vary by more than one order of magnitude. For aerosol particles in the 500 nm to 2.5 μm size range, significant correlations were found between the two sampling methods, resulting in correlation coefficients (r^2) ranging from 0.22 to 0.93. In addition, transient fluctuations in aerosol counts on a timescale of 5 to 10 minutes were successfully observed simultaneously with the two monitoring techniques, thereby demonstrating the temporal resolution of LIBS.

Index Headings: Laser-induced breakdown spectroscopy; LIBS; Aerosol; PM_{2.5}; Ambient air.

INTRODUCTION

Measurement of ambient air particulate matter presents one of the more challenging problems in analytical instrumentation as related to overall environmental monitoring. While aerosols themselves comprise a diverse and constantly fluctuating system, monitoring needs may vary from total mass loadings and total aerosol counts (i.e., number density), to more complicated needs like detailed breakdowns of elemental content by aerosol size fractionation. Furthermore, the elemental analysis of particulate matter is made more difficult by the variation in particle size and the complex nature of aerosol matrices. For example, soot particulates are on the order of tens to hundreds of nanometers in size and contain carbon as the dominant elemental fraction. Additionally, dust- or mineral-rich particles may extend to many micrometers in diameter and contain multiple elements including a range of metallic compounds, while bioaerosol particles contain a range of organic matrices characterized by many potential trace species. Therefore, ideal characteristics of an ambient aerosol monitoring instrument include the ability to analyze individual particles for size and composition, while providing for rapid or real-time *in situ* analysis. Toward this end, two primary techniques have been used to analyze individual airborne particles in real time: laser-induced breakdown spectroscopy

and laser-desorption–time-of-flight mass spectrometry. The latter technique is perhaps the more mature of the two and has been reported in a number of studies.^{1–5} The former, however, enjoys many characteristics suited to analysis of ambient air particulate matter and will form the basis of the current study.

Laser-induced breakdown spectroscopy (LIBS), also known as laser-induced plasma spectroscopy (LIPS), is an atomic emission spectroscopy technique that uses a pulsed laser beam to produce a laser-induced breakdown or plasma. For the application of aerosol analysis, the breakdown may be produced directly in the sample stream, where it serves as both the sample volume and the excitation source, thereby dissociating all molecules and fine particulates within the highly energetic microplasma. The resulting plasma emission can be collected and resolved both spectrally and temporally to yield spectra containing the atomic emission lines corresponding to the atoms present in the plasma volume, including elements originating from within aerosol particles effectively sampled by the plasma. LIBS, as discussed below, is an analytical technique that is sensitive enough for measuring aerosol elemental composition, while also functioning as a real-time *in situ* monitor.

The LIBS technique has been applied successfully in a number of studies for the determination of overall elemental mass concentrations, including several studies addressing continuous on-line monitoring of air emissions and aerosol.^{6,7} Other research and review papers focusing on LIBS are reported in the literature.^{8–11} An extension of the LIBS technique for real-time sizing and elemental analysis of single aerosol particles based on the analysis of individual LIBS spectra was reported in a series of papers.^{12,13} The technique has proven to be both robust and highly sensitive during a range of reported field measurements, including detection of ambient aerosol,¹² ambient aerosol and observed atmospheric fluctuations associated with the discharge of fireworks,¹⁴ and PM measurements made as part of a larger, multi-instrument campaign at an EPA-funded air quality site.¹⁵ These studies have demonstrated the feasibility and sensitivity of LIBS for analysis of ambient air particulate matter, including single-particle analysis. In support of such efforts, a number of related studies have examined the analytical aspects of the LIBS technique, including an analysis of sampling statistics with respect to analyte signal optimization,¹⁶ the effects of temporal and spectral plasma size and stability, including the role of aerosols,^{17,18} the investigation of aerosol size effects for quantitative analysis,¹⁹ and the statistics and optimization of single-particle detection algorithms as implemented for LIBS-based conditional analysis.²⁰

While the application of laser-induced breakdown spectroscopy to quantitative aerosol analysis has been realized, the rich problem of ambient aerosol monitoring remains in need of

Received 19 July 2005; accepted 30 December 2005.

* Author to whom correspondence should be sent. E-mail: dwhahn@ufl.edu.

additional research. To date, the two most relevant studies by Carranza et al. in 2001¹⁴ and Lithgow et al. in 2004¹⁵ have reported LIBS spectra representative of individual particles and have tracked fluctuations in speciated aerosol concentrations. However, no study has provided a detailed assessment that is focused on real-time LIBS-based ambient aerosol analysis in combination with simultaneous, independent particle analysis. Such a study forms the basis for this paper, with the goal of further understanding and assessing the efficacy of the LIBS technique for quantitative analysis of aerosol systems, notably ambient air particulate matter.

EXPERIMENTAL METHODS

Aerosol Sampling System. For all analyses, ambient air was sampled using a PM_{2.5} sampling inlet (Rupprecht and Patashnick) operating at a constant sampling rate of 1 m³/h. The sampling inlet was positioned about 5 m above the ground on a 1 m wide concrete ledge adjacent to a three-story building. The air was transferred from the sample inlet to the particle sampling chamber (see Fig. 1) using a 10 m long sample line constructed from 11.4 mm i.d. seamless stainless-steel tubing. The entire transfer line was designed to minimize particle loss, namely loss via particle diffusion and impaction to the tubing walls. To quantify such losses, the entire configuration was modeled using a particle deposition code,²¹ which yielded transfer efficiencies ranging from 98.2% for the 100 nm particles to 78% for 2.5 μm particles, with a mean of 91.4% over the entire size range and a mean of 90% between 0.5 and 2.5 μm. It is noted that guidelines are available for overall placement of inlets for ambient air sampling (e.g., distance from structures). However, no additional modeling or calculations were performed with respect to the overall placement of the PM_{2.5} inlet, as the goal of the present study was a *relative comparison* of a sampled ambient air aerosol stream, rather than

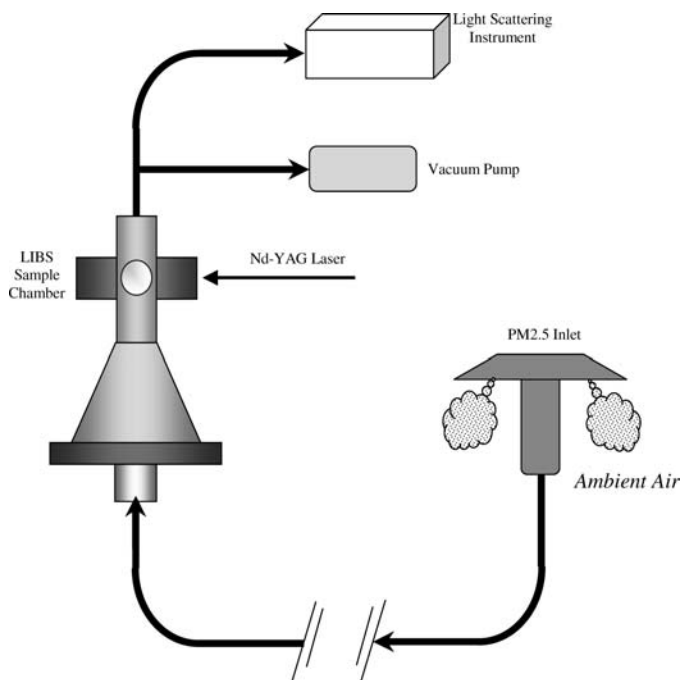


FIG. 1. Ambient air collection apparatus. Ambient air is drawn through a PM_{2.5} sampling inlet to the LIBS sample chamber and to a commercial light scattering instrument.

an absolute total particle count. As such, the presented aerosol data were not corrected for any aerosol transport efficiencies between the PM_{2.5} inlet and the sampling chamber.

Figure 1 shows a schematic of the aerosol sampling arrangement, including the sample stream bifurcation for sample delivery to the total aerosol sampling instrument (i.e., light scattering instrument). A vacuum pump was used to provide the bulk sampling flow rate from the PM_{2.5} inlet through the LIBS sample chamber. The pressure drop through the overall sample system (PM_{2.5} inlet to LIBS sample chamber) was minimal, with the pressure in the LIBS sample chamber reduced by only about 1 cm of water (as measured) with respect to ambient air pressure. A split line (separation tee) was installed between the LIBS sample chamber and the vacuum pump to enable sampling of the air flow by the total aerosol monitoring instrument, which is described in detail below. The light scattering instrument contained an additional vacuum pump that sampled at a fixed flow rate of 280 cc/min. The tee was arranged (see Fig. 1) such that the sample stream to the total aerosol instrument (light scattering device) was passed straight through the tee to avoid the sharp bend. The transfer line from the LIBS chamber to the total aerosol instrument was constructed from less than 1 m of 3/8-inch polypropylene tubing, with an i.d. of 6.4 mm.

Laser-Induced Breakdown Spectroscopy Analysis. A brief overview of the LIBS experimental setup and aerosol analysis scheme is presented here, with additional details reported previously.^{13,14,22} The excitation source was a 1064 nm Q-switched Nd:YAG laser with a nominal pulse width of 10 ns, laser pulse energy of 275 mJ, and operated with a 5 Hz pulse repetition rate. The expanded laser beam (12 mm diameter) was focused into the sample chamber using a 75 mm ultraviolet (UV)-grade plano-convex lens to create the plasma at about the center line of the six-way cross that formed the LIBS sample chamber. The plasma emission was collected along the incident beam in the backward direction (180°) and separated using a pierced mirror. The plasma was formed with sufficient laser pulse energy to achieve saturation with respect to absorbed pulse energy, which results in enhanced shot-to-shot precision as previously reported,¹⁶ while the collection geometry (i.e., backscatter mode) was designed to minimize spatial variability. The collected plasma emission was fiber-coupled to a 0.275-m spectrometer, dispersed with a 2400 grooves/mm grating (0.03 nm/pixel, 0.12 nm resolution), and recorded with an intensified charge-coupled device (iCCD) detector array.

In the present study, two analyte species were selected for identification of ambient air particles, namely calcium and sodium. Detection of these two elements was performed using two ionic calcium atomic emission lines at 393.37 nm (0–25 414 cm⁻¹) and 396.85 nm (0–25 192 cm⁻¹), and using the sodium doublet at 589.00 and 589.59 nm (0–16 973 and 0–16 956 cm⁻¹). These emission lines have been successfully employed for LIBS-based analysis of ambient aerosol particles on several occasions.^{12,14,15} For all spectral data acquisition, a delay of 40 μs with respect to the incident laser pulse was used followed by an integration width of 40 μs. Such a gate was found to provide an optimal ratio of atomic emission to continuum emission by allowing time for the pronounced continuum emission to decay.

As reported in an earlier study,¹⁴ the expected LIBS-based sampling rate (defined as the percentage of total laser shots that

sample a targeted particle type) for calcium-based and sodium-based ambient air particles is on the order of 0.1 to 1%. To overcome the low analyte signal-to-noise ratio associated with ensemble averaging at such limited sample rates, conditional signal processing was employed. LIBS-based conditional processing entails examining each spectrum for the presence of a distinct atomic emission peak (or peaks) corresponding to the target analyte. All spectra characterized by pronounced analyte emission are classified as a particle "hit" and subsequently saved. Suitable approaches for single-shot detection of ambient air particulates have been reported in previous studies,^{13,14,23} while a detailed study of conditional spectral processing in the context of spectral noise and false hit rates was reported in a more recent study.²⁰ For the current work, the peak-to-base (P/B) ratio was calculated in real time using the calcium or sodium emission lines for each recorded spectrum. The P/B ratio was calculated by averaging the intensity over seven pixels (~0.2 nm full width) centered about the expected emission line and then dividing by the average intensity of a baseline region selected to avoid any interfering atomic emission peaks. For the relatively flat background region near the calcium and sodium emission lines, the resulting P/B signal was about unity in the absence of any analyte emission. A suitable P/B threshold value was selected by steadily increasing the threshold until a desired number of false hits (i.e., hits in the absence of any analyte) was realized. This was done through HEPA-filtered air. The optimal false hit rate depends on the ultimate data processing needs, with trade-offs in spectral noise and expected false hit rates, as discussed in detail in an earlier study.²⁰ In the present study, a significant experimental parameter was the target particle hit rate, and hence it was important to minimize (essentially eliminate) false hit rates. To accomplish this, a threshold value was set at about 100% above the average P/B ratio recorded in the absence of any analyte, which typically produced zero to one false hit for two to three thousand laser shots.

For calibration, aerosol streams were generated by nebulizing (0.11 mL/min) aqueous analyte solutions of deionized water, or dilutions of stock 10 000 µg/mL sodium or calcium in water, into a gaseous co-flow stream of purified, dry air. The stock aqueous solutions were diluted using ultra-purified water to produce a desired range of analyte concentrations directly in the LIBS sample chamber. Air was collected and compressed from the air-conditioned laboratory building and then passed through a water separator, particle filter, pressure regulator, desiccant drier, and a final high-efficiency particulate (HEPA) filter prior to entering the flow controllers and sample chamber. For both calcium and sodium, the resulting calibration curves were highly linear, with correlation coefficients (*r*) greater than 0.99.

Light Scattering Analysis. The total aerosol counts were determined using a commercial light scattering based instrument (LASAIR-1001, PMS Inc., Boulder, CO). The light scattering instrument provided no chemical information about the measured aerosol species, but rather the equivalent light scattering based diameter. The instrument output was divided into eight size bins, which correspond to the following particle sizes: 0.1–0.2 µm, 0.2–0.3 µm, 0.3–0.4 µm, 0.4–0.5 µm, 0.5–0.7 µm, 0.7–1.0 µm, 1.0–2.0 µm, and >2.0 µm. In view of the PM_{2.5} inlet, the last channel effectively measured particles in the size range from 2.0 to 2.5 µm. The instrument was configured to provide total aerosol counts for each size bin for 5-minute sampling periods. Noting that the total gas sampling

rate was equal to 280 cc/min, the 5-minute sample periods corresponded to a total ambient air sampling volume of about 1.4 liters through the light scattering instrument.

RESULTS AND DISCUSSION

Laser-Induced Breakdown Spectroscopy-Based Spectral Processing. The primary goal of the present study is to examine the correlation between LIBS-based speciated aerosol measurements and light scattering based total aerosol counts, thereby assessing the statistical basis for conditional spectral processing and quantitative aerosol analysis in the context of ambient air monitoring. To support this goal, a series of measurements was performed over an approximate 5-week period between July 2 and August 6. During this period, 60 1-hour sampling periods were analyzed, during which simultaneous light scattering and LIBS-based aerosol measurements were recorded. For each 1-hour sampling period, light scattering data was continually recorded using sequential 5-minute sampling intervals. In addition, for each 5-minute sampling interval, a 1500 shot LIBS spectral sequence (5 Hz pulse rate) was simultaneously recorded and analyzed in real time for the presence of either sodium or calcium. Because sodium and calcium emission could not be measured simultaneously with the approximately 30 nm spectral bandwidth of the spectrometer/iCCD system, the 1-hour sampling periods were alternated between sodium- and calcium-based aerosol analysis. The 1-hour sampling periods were spaced throughout the 5-week period, with generally two to four 1-hour periods recorded per day. All sampling periods were recorded between 11:30 AM and 9:30 PM, and in the absence of any rain.

For each 1-hour sampling period, all of the spectra corresponding to a particle hit were ensemble-averaged together to yield a single spectrum representative of the targeted analyte-containing aerosol particles. In addition, all 18 000 of the spectra recorded during the 1-hour period (including identified hits) were ensemble-averaged to yield a representative average spectrum corresponding to the ambient air. As an example of this process, two spectra corresponding to the ensemble average of all shots and the ensemble average of all calcium-based hits are presented in Fig. 2, as recorded between 12:20 and 1:20 PM on July 2. The two spectra are presented as recorded and averaged, with no scaling between the two curves. During this period, 187 calcium-based particle hits were recorded, which resulted in a significant calcium emission signal, as observed in the figure. Several features in the figure are noted, including the near-perfect overlap of the two spectra over the entire wavelength range, with the exception of the pronounced calcium emission lines. Essentially, the perfect agreement between the two spectra supports the independence of the overall plasma emission processes on the presence or absence of the calcium-based aerosol particles. Detailed comments are offered below on the overall signal strength (e.g., effective calcium concentration) of the calcium emission line; however, it is readily apparent that the calcium emission signal is below the detection limit in the ensemble average of all shots. In contrast, the two calcium emission lines at 393.4 and 396.9 nm display an excellent signal-to-noise ratio in the conditional-processed average spectrum, thereby demonstrating the analytical value of such an approach for the analysis of discrete and rare emission events such as aerosol sampling, as realized with the calcium-based particles. Several

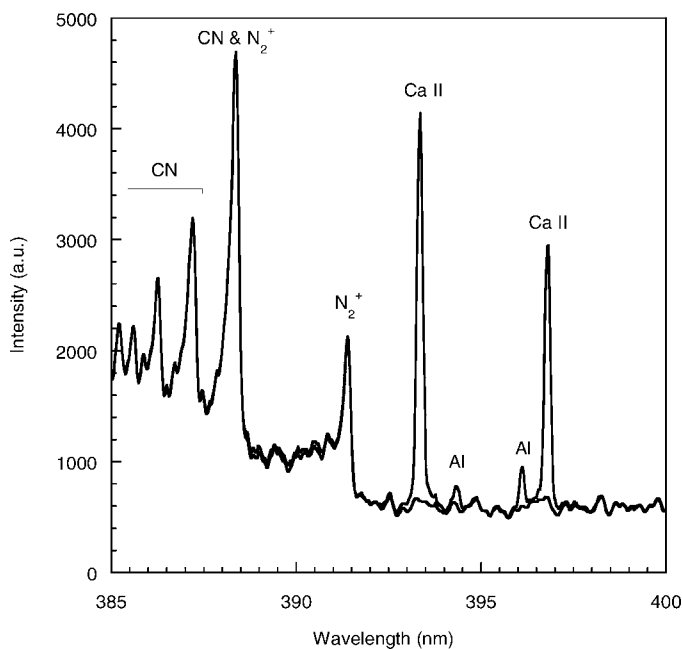


FIG. 2. 18 000-shot ensemble-averaged spectrum recorded for a 1-hour sampling period along with an average of 187 shots corresponding to calcium-based particle hits. The spectrum of calcium hits is identifiable by the pronounced calcium emission lines. Both spectra have the same intensity scale.

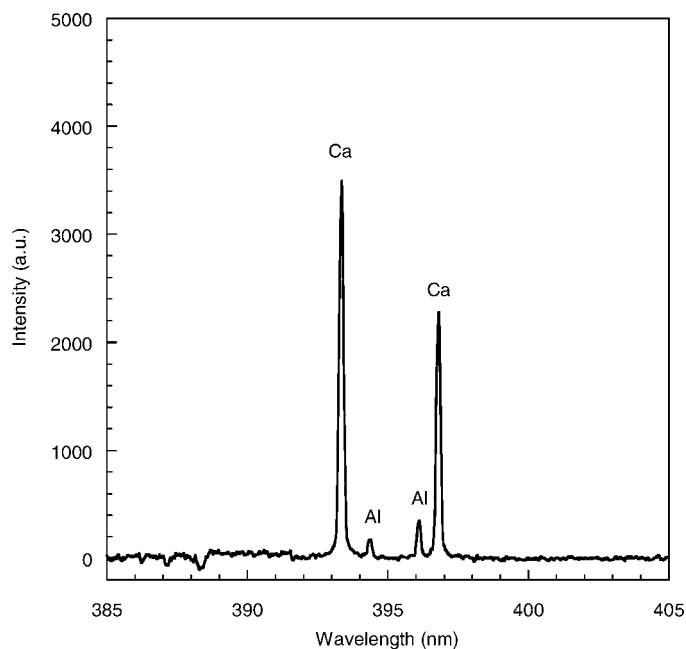


FIG. 3. Background-subtracted spectrum corresponding to Fig. 2. The spectrum represents the subtraction of the 18 000-shot ensemble average from the average spectrum of the 187 calcium-based particle hits.

additional features are noted and labeled in the two spectra, namely the pronounced emission features at 391.4 and 388.4 nm, which are attributed to the N_2^+ first negative system,²⁴ and the band head corresponding to the CN violet system (primarily at 388.3 and 387.1 nm), noting that the line at ~ 388 nm is a combination of these two molecular lines. Subtraction of the two raw waveforms in Fig. 2 results in a single spectrum indicative of the targeted analyte lines, namely the calcium lines, as shown in Fig. 3. Note that two aluminum I lines at 394.4 and 396.2 nm are also present in the background-subtracted spectrum. While the conditional processing algorithm was targeted only on calcium for this data set, the appearance of aluminum emission is evidence of a subset of aerosol particles rich in both calcium and aluminum.

Before attempting to correlate the recorded light scattering based sampling rates with the LIBS-based particle hit rates, as discussed below, one should first consider the LIBS data in terms of the expected sensitivity and lower detection limits for the two analytes. The LIBS spectrum shown in Fig. 3 corresponds to an average of 187 individual calcium-rich aerosol hits. The resulting average calcium-based aerosol number density can be estimated by the quotient of the measured LIBS-based sample rate (187/18 000) and the effective plasma sampling volume of 1.17 mm^3 , as reported previously.²⁵ This yields an average calcium-based particle number density equal to approximately 9 particles/cm^3 , corresponding to the Fig. 2 data. Furthermore, based on the analyte response of the Fig. 3 spectrum (per the calibration curve) and the measured particle number density, the average calcium analyte mass per particle is equal to about 50 fg. If one models the average calcium-based aerosol as calcium carbonate, with a density of 2.7 g/cm^3 and calcium mass fraction of 0.40, 50 fg of calcium corresponds to an average particle diameter of about 450 nm. Ambient air particulates rich in calcium are mostly attributed to calcium carbonate or gypsum,

although significant numbers of CaSO_4 particulates may also be present that stem from anthropogenic sources.^{26,27} Using the conditional analysis routine as implemented, along with the calcium calibration curve and the corresponding spectral noise, it is estimated that the lower detection limit for single particle analysis was about 10 fg in the current study, corresponding to an equivalent calcium carbonate particle diameter of 275 nm. In a similar manner, sodium-based detection limits are estimated as about 20 fg, corresponding to an equivalent sodium chloride particle of 350 nm. Earlier studies reported detection limits on the order of 1 fg for calcium and 2–3 fg for sodium-based ambient aerosols, while in a recent study, calcium was successfully recorded in aerosolized bacillus spores at absolute mass levels approaching a single femtogram.²⁸ It is noted that the bacillus study utilized automated conditional processing for preliminary spectral screening, followed by rigorous manual inspection to finally identify genuine analyte signals at the fg level. In the present study, a fully automated conditional processing scheme was the sole means of spectral processing, with the hit thresholds set relatively high to minimize any false hits due to spectral noise fluctuations. While a statistical analysis of the individual spectra corresponding to particle hits was not the focus of the current study, several of the larger single-shot spectral signatures observed yielded an absolute calcium mass near 1000 fg, which corresponds to a calcium carbonate particle 1.2 μm in diameter. Such a particle is within the limits expected for complete particle vaporization and linear analyte response, based on recently measured upper size limits of about 2 μm for silica microspheres under nearly identical experimental conditions.¹⁹ Taken in concert, the above comments indicate that a wide range of calcium-based and sodium-based aerosol particles were simultaneously assessable with the LIBS technique and the light scattering instrument over the measurable size range from a few hundred nanometers up to about 2.5 μm .

Correlation of Laser-Induced Breakdown Spectroscopy and Light Scattering Results. The data corresponding to Figs. 2 and 3 are characterized by a total of 187 laser particle hits, as based on calcium emission, out of the total of 18 000 shots during the 1-hour sampling period. This yields a calcium-based aerosol sampling rate of almost exactly 1%, which nominally corresponds to a two-order-of-magnitude enhancement in analyte signal-to-noise ratio, assuming that the spectral shot noise is averaged to its intrinsic limit after more than about 100 spectra. The particle hit rate may be linked to the particle number density via the Poisson distribution, as described previously.¹³ Specifically, for low sampling rates, the sampling rate S is given as

$$S = V_p N \quad (1)$$

where V_p is the effective plasma sampling volume and N is the particle number density. Therefore, with a constant effective plasma sampling volume, the LIBS-based particle sampling rate (i.e., hit rate) is directly proportional to the number density of the targeted particles. While LIBS aerosol sample rates have been reported in several studies,^{14,15} to date, no study has provided a real-time comparison with independently measured, total (i.e., non-spectiated) aerosol particle counts. The light scattering data were used to provide such a comparison.

The light scattering data are summarized in Table I for the 30 1-hour sampling periods that correspond to the LIBS-based calcium-rich aerosol measurements. With the light-scattering data recorded in 5-minute sample intervals, the 30 sampling periods correspond to a total of 360 individual 5-minute measurements. As expected, the data show a continuous decrease in total particle count rates with increasing particle size range. The maximum average particle count rate was slightly over 200 000 particle counts/min in the particle size range from 100–200 nm, while the minimum average particle count rate was 15 counts/min in the 2–2.5 μm range. For all size ranges, considerable variation was observed over the 5-week sample period, with all size bins except the finest yielding an order of magnitude variation in particle count rate and with relative standard deviations ranging from 46% to 106%, as based on the 30 1-hour sampling periods.

Figure 4 presents a plot of the LIBS-based calcium particle sampling rate (i.e., number of calcium containing spectra as a percentage of total spectra) and the light scattering based total aerosol sampling rate for the cumulative size range between 500 nm and 2.5 μm for the 30 1-hour sampling windows. The overall correlations are quantified below, but the excellent tracking of the LIBS-based and total aerosol counts is noted over a range of aerosol loadings that varied by more than one order of magnitude. The LIBS data may be readily converted to

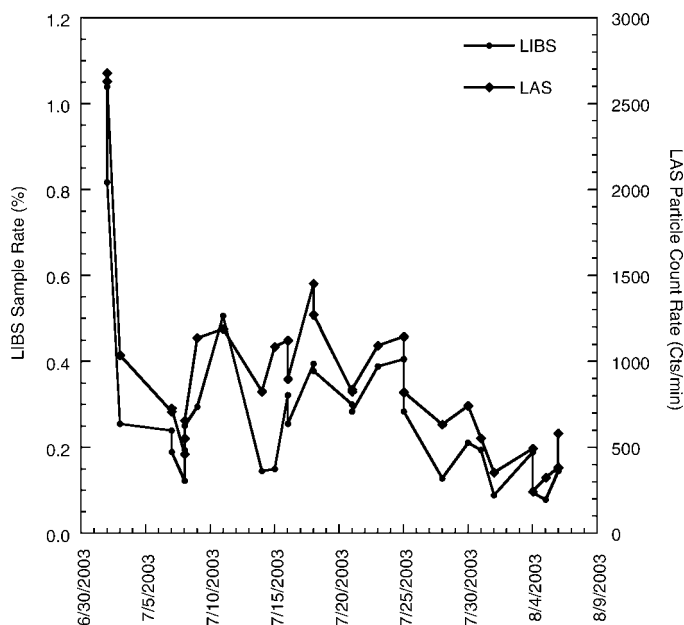


Fig. 4. LIBS calcium-based particle sampling rate (calcium-containing spectra/total spectra) and the light scattering based (LAS) total aerosol sampling rate for the cumulative size range between 500 nm and 2.5 μm . The data are presented for thirty 1-hour sampling intervals.

a calcium-based aerosol number density through the use of Eq. 1, namely by multiplying by the effective plasma sample volume. Similarly, the light scattering data may be converted to total aerosol densities using the aerosol sampling rate (280 cc/min). Direct comparisons of aerosol number densities between the two methodologies are presented below; however, one must consider uncertainties in the LIBS sample volume and the overall counting efficiency of the light scattering instrument. As such, the raw data (i.e., particle hit rates and particle counts, respectively) will be used to examine the correlation of the two techniques. The comparison of LIBS-based sodium particle sampling rates and the light scattering sampling rates (500 nm to 2.5 μm size range) are presented in Fig. 5 for the corresponding 30 1-hour sampling periods. As with the calcium results, a degree of correlation between the two methods is observed, although more variation is apparent with Fig. 5 as compared to Fig. 4.

To quantify the correlation between the LIBS and light scattering aerosol measurements, the pairs of LIBS and light scattering data were directly plotted for each size bin of the light scattering instrument. A representative case is presented in Fig. 6, which presents the LIBS-based calcium-containing particle hit rate plotted against the light scattering based aerosol

TABLE I. Light scattering sampling statistics for ambient aerosol as measured for 360 5-minute sample intervals.

Particle size (μm)	Avg. sample rate (cts/min)	Max. sample rate (cts/min)	Min. sample rate (cts/min)
0.1–0.2	202 093 (46% ^a)	577 695	71 818
0.2–0.3	58 631 (57% ^a)	165 713	17 723
0.3–0.4	13 597 (91% ^a)	65 751	3 006
0.4–0.5	2 070 (106% ^a)	11 666	391
0.5–0.7	442 (54% ^a)	1 117	107
0.7–1.0	260 (73% ^a)	921	60
1.0–2.0	199 (78% ^a)	763	39
2.0–2.5	15 (104% ^a)	77	2

^a Relative standard deviation.

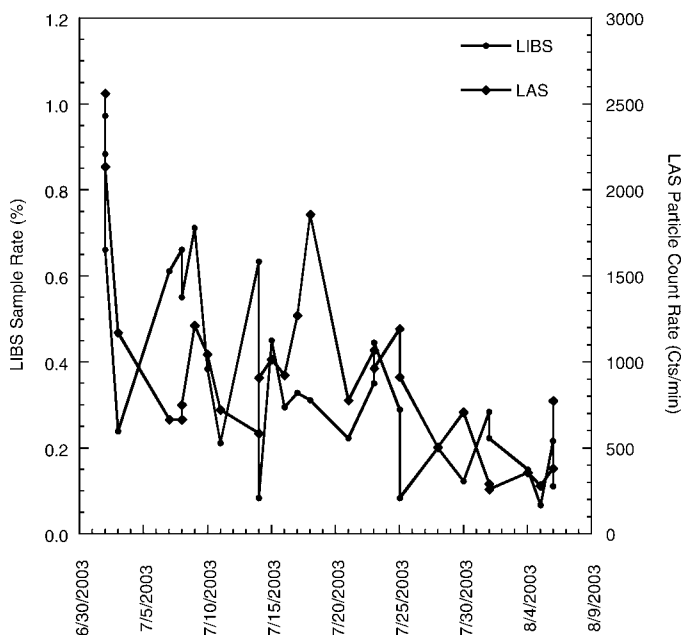


FIG. 5. LIBS sodium-based particle sampling rate (sodium-containing spectra/total spectra) and the light scattering based (LAS) total aerosol sampling rate for the cumulative size range between 500 nm and 2.5 μm . The data are presented for thirty 1-hour sampling intervals.

counts in the 1–2 μm size bin. A linear regression curve is also shown in the figure, which yields a regression coefficient (r^2) equal to 0.931. Similar curves were prepared for each of the light scattering instrument size bins, for both the calcium and sodium-based LIBS measurements. Table II provides a summary of the regression coefficients for all cases. Two observations are noted in the Table II data. First, for both the sodium- and calcium-based measurements, there is marked decrease in the regression coefficients corresponding to the light scattering based particle size ranges below 0.5 μm . The cause of this precipitous drop in correlation is concluded to be two-fold, due in part to the significant increase in total particle counts below about 0.5 μm , as observed in Table I, and hence is not unexpected that calcium- and sodium-based aerosol particles become a smaller percentage of the total. Secondly, recall that the current LIBS-based detection limits for these two aerosol types were estimated to be on the order of 300–400 nm (depending on the exact particle composition and analyte mass fraction). In consideration of Table II, the overall LIBS and light scattering correlations presented above in Figs. 4 and 5 were based on the total aerosol counts (light scattering) in the size range between 0.5 and 2.5 μm , consistent with the above comments. The second observation in the Table II data is that for all data in the 0.5 to 2.5 μm range, the calcium-based LIBS-data were found to correlate better (i.e., greater regression coefficient) with the light scattering data. To better explore this latter observation, it is useful to calculate the overall aerosol loadings based on the two measurement techniques.

As described above, the speciated aerosol number density (i.e., LIBS-based) is readily calculated from the measured particle sampling rate as described by Eq. 1. Using the LIBS sampling volume of 1.17 mm^3 , as previously reported for similar experimental parameters, the aerosol number densities were calculated for both the calcium-based and sodium-based LIBS data. The average LIBS-based particle number densities over the 30 1-hour sampling periods are 2.0 $\text{particle}/\text{cm}^3$ (89%

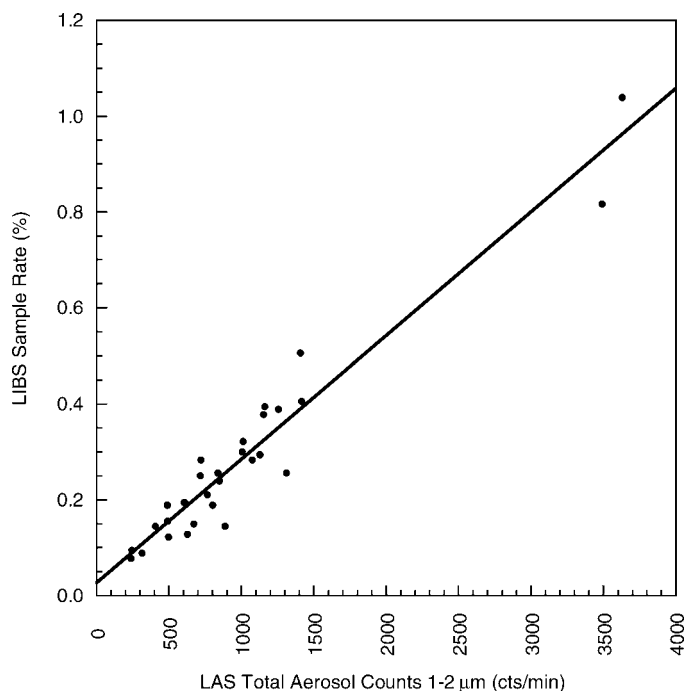


FIG. 6. LIBS calcium-based particle sampling rate as a function of light scattering based particle counts in the size range of 1 to 2 μm . Data correspond to thirty 1-hour sampling periods. Results of the linear regression are provided in Table II.

RSD) and 2.8 $\text{particles}/\text{cm}^3$ (76% RSD) for calcium-based and sodium-based detection, respectively. To more accurately calculate the speciated number densities, the expected contribution of false hits was subtracted from the total number of recorded hits based on the threshold values used for triggering hits. As discussed above, the threshold was adjusted to produce a false hit (with no analyte present) about every 2000 laser shots. Hence, for the 1-hour sampling periods, a total of 9 false hits would be expected for the corresponding 18 000 laser shots.

To put the LIBS-based aerosol number densities in the context of the total aerosol counts as measured with the light scattering instrument, the percentage of speciated aerosol counts to total aerosol counts was evaluated for the calcium-based and sodium-based data. The total aerosol number densities (size range between 0.5 and 2.5 μm) were readily calculated from the total light scattering based particle counts per minute divided by the total sample volume per minute (280 cm^3). The average aerosol number density in this size range

TABLE II. Regression coefficients for linear correlation of light scattering based and LIBS-based aerosol measurements over 30 1-hour sampling periods.

Light scattering particle size (μm)	LIBS calcium-based (r^2)	LIBS sodium-based (r^2)
0.1–0.2	0.013	0.000036
0.2–0.3	0.000054	0.00000043
0.3–0.4	0.00066	0.0043
0.4–0.5	0.0092	0.0038
0.5–0.7	0.66	0.22
0.7–1.0	0.93	0.47
1.0–2.0	0.93	0.51
2.0–2.5	0.91	0.39

was about 7 particles/cm³ (62% RSD), which agrees well with reported size-based aerosol loadings in ambient air.²⁹ To allow a valid comparison between the measured calcium-based and sodium-based number densities, the two data sets were paired such that back-to-back sample periods (1-h sample of sodium-based data followed by a 1-h sample of calcium-based data, or vice versa) were grouped with a time-stamp corresponding to the middle of the sampling period. Because sodium- and calcium-based monitoring were not always conducted together, the 30 1-hour sampling periods of each species resulted in 22 back-to-back 2-hour sampling periods, with the resulting data presented in Fig. 7. As expected, the relative contributions of the sodium-based and calcium-based particles to the total aerosol counts are observed to fluctuate significantly over the 6-week sampling period. The average calcium-based aerosol percentage was 26% (38% RSD), and the average sodium-based aerosol percentage was 38% (68% RSD), with a maximum percentage of 44% and 97%, respectively. Given the likelihood that a significant fraction of the recorded sodium-based aerosols are marine related (e.g., sea salt particulates), it is not surprising to see a larger fluctuation in the contribution of sodium-based aerosols, due for example to the prevailing winds across the Florida peninsula. It is noted that the sampling location is located approximately equal distances from the Atlantic coast and the Gulf of Mexico.

Several important observations may be made from Fig. 7. First, it is noted that the average sum of the calcium- and sodium-based aerosol loadings are about 64% (41% RSD). Assuming that the speciated and total aerosol loadings did not vary significantly over the typical two-hour sampling period, the combined data sets show that these two species account for

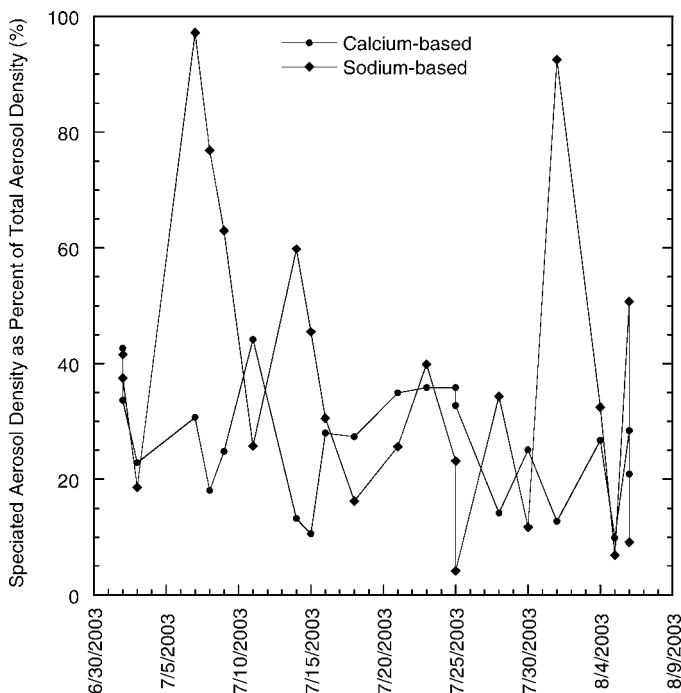


FIG. 7. LIBS-based speciated aerosol number density as percentage of the light scattering based total aerosol number density in the cumulative size range between 500 nm and 2.5 μm . Speciated data are presented for both calcium-based and sodium-based hits.

about two-thirds of the aerosol species in the size range from 0.5 to 2.5 μm . One must caution that no recent independent calibration of the light scattering instrument for total aerosol counts (i.e., counting efficiency) was performed, although auxiliary measurements suggest agreement within a factor of two between actual aerosol densities in the sample stream and the expected corresponding instrument counts. Despite the experimental uncertainties, clearly the speciated aerosols (i.e., sodium- and calcium-based) were a significant fraction of the total aerosol loadings in this particular size range, which explains the excellent correlation between LIBS-based and light scattering based aerosol counts, as observed in Figs. 4 through 6 and summarized in Table II. Finally, a few words are noted about the potential correlation between the sodium-based and calcium-based LIBS particle hits. While the current spectrometer system did not enable simultaneous detection of the calcium and sodium atomic emission lines, one can still examine the correlation between the two species for the paired one-hour samples. If the sodium and calcium species were largely common to a single aerosol particle, then one would expect a significant correlation between the speciated percentages of total aerosol counts. A plot of the calcium-based percentages against the sodium-based percentages revealed no discernable correlation, with a linear regression coefficient of 0.037 (r^2). The data support the conclusion that the calcium- and sodium-based aerosol particles contain a significant fraction from different aerosol compounds, with the former expected from minerals such as calcium-carbonate or perhaps dolomite, and the latter expected from sea-derived aerosol, with a possible contribution from sodium nitrate particulates.

Laser-Induced Breakdown Spectroscopy Temporal Resolution. The data and discussion reported above are all based on 1-hour sampling periods. Such sample periods correspond to 18 000 laser shots and were found to produce nearly 200 particles hits at times. As noted above, LIBS-based particle analysis is ultimately an exercise in statistical sampling, and such sample intervals generally provide valid statistics. For example, in one of the earlier studies on LIBS-based aerosol analysis, it was concluded that some tens of particles can provide valid statistical samples based on numerical simulations and experimental measurements.²³ However, it is also useful to explore the temporal resolution that may be realized with the LIBS methodology in the current study. Figures 8 and 9 present the LIBS-based and light scattering based sample rates (0.5 to 2.5 μm) for a single 1-h sampling period for calcium- and sodium-based monitoring, respectively. In both figures, the individual data points represent 5-minute averages, which corresponds to 1500 laser shots for the LIBS data, and a sample volume of 1350 cm³ for the light scattering instrument.

The calcium data set in Fig. 8 reveals a total particle count (light scattering based) that was essentially constant during the 1-h sample period. Specifically, the average count rate was 2676 min⁻¹, with a relative standard deviation of only 1.5%. The LIBS data are also quite consistent about the 1-h average value of 1.03%; however, the relative standard deviation is increased to 19.6%. The calcium data were selected to correspond to one of the higher hit rates observed for a 1-h period, with an average of 15.6 particle hits recorded per 5-minute, 1500-shot sequence. As mentioned in the above comments, tens of particle hits become a sufficient sample size to accurately predict the average particle hit rates.²³ The nearly

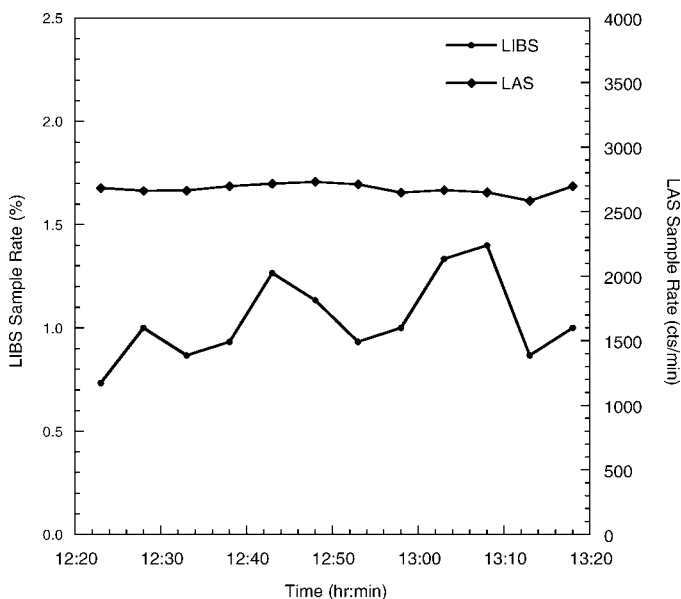


FIG. 8. LIBS calcium-based particle sampling rate (calcium-containing spectra/total spectra) and the light scattering based (LAS) total aerosol sampling rate (0.5 to 2.5 μm) for a single 1-hour sampling period. Each data point represents a 5-minute interval, which corresponds to a 1500 shot LIBS sequence. The horizontal line represents the 1-hour LIBS average.

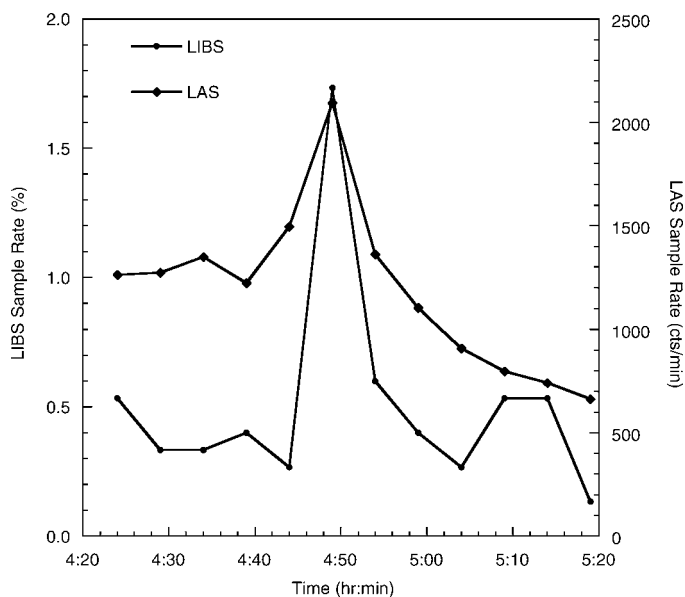


FIG. 10. LIBS calcium-based particle sampling rate (calcium-containing spectra/total spectra) and the light scattering based (LAS) total aerosol sampling rate (0.5 to 2.5 μm) for a single 1-hour sampling period. Each data point represents a 5-minute interval, which corresponds to a 1500 shot LIBS sequence.

16 particle hits per 5-minute sequence is consistent with this value, although toward the lower bound, which therefore corroborates the ability of LIBS-based sampling to track aerosol number density with rather detailed temporal resolution provided sufficient particle hits are recorded. Interestingly, it is noted that the previous numerical simulations predicted a standard deviation of 17% for total particulate mass

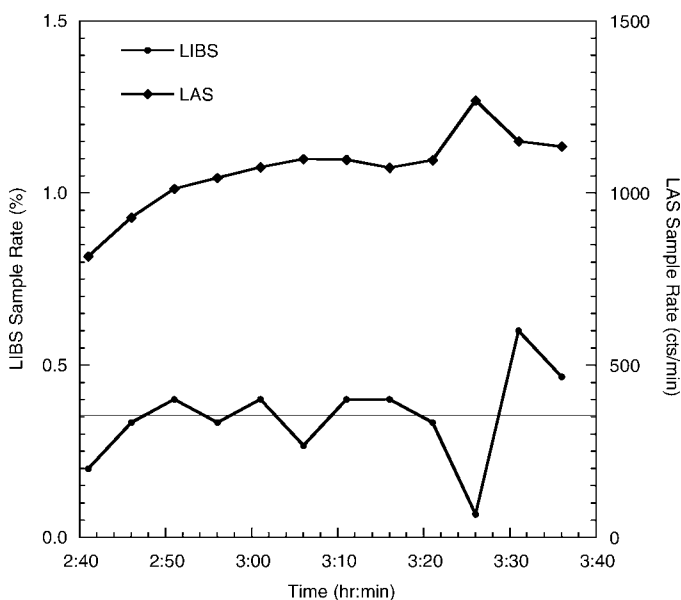


FIG. 9. LIBS sodium-based particle sampling rate (sodium-containing spectra/total spectra) and the light scattering based (LAS) total aerosol sampling rate (0.5 to 2.5 μm) for a single 1-hour sampling period. Each data point represents a 5-minute interval, which corresponds to a 1500 shot LIBS sequence. The horizontal line represents the 1-hour LIBS average.

monitoring, corresponding to an average sampling rate of 17 particles per interval,²³ which agrees surprisingly well with the current study. The sodium-based LIBS data presented in Fig. 9 also display a consistent correlation with the total aerosol counts over the 1-h sample period. Both data sets display a modest initial rise that somewhat reaches a plateau toward the end of the sample period. The average total particle count rate is 1066 min^{-1} (10.6% RSD), while the average LIBS-based hit rate is 0.35% with a 35% RSD. The relative standard deviation of the Fig. 9 LIBS data is nearly twice the value of the Fig. 8 data; however, the average number of particle hits per 5-minute interval was decreased to 5.3 particles for the latter data, as compared to the value of 15.6 reported for Fig. 8. It is therefore expected that the fluctuation in measured sample rate per 5-minute interval should increase given the essentially sample-limited conditions (i.e., less than the desired 10–20 particle hits per interval).

A final data set is reported that further demonstrates the temporal resolution of LIBS for ambient aerosol monitoring. Figure 10 shows a single 1-hour sampling period corresponding to LIBS data based on calcium monitoring, along with the total aerosol counts based on light scattering. As discussed above, each data point represents a 5-minute sample period. As observed in the figure, about halfway through the sample period, there was a significant increase in the aerosol concentration. Specifically, the light scattering based sample rate increased from an average value of about 1200 cts/min to more than 2100 cts/min over a 10-minute period. Similarly, the calcium-based LIBS particle sampling rate increased approximately four-fold from a 0.4% average sampling rate to 1.7% over the corresponding 5-minute sample interval. Such temporal response with LIBS has been demonstrated before with emissions monitoring in an effluent stack,³⁰ however, never has such temporal resolution been demon-

strated and independently corroborated with ambient air particulates.

CONCLUSION

Laser-induced breakdown spectroscopy is a promising technique for real-time analysis of aerosol particles. Such an analytical method has many applications, of which ambient air analysis is particularly well-suited given the particle size range of primary interest (e.g., PM_{2.5}) and the typical aerosol loadings that make single-particle analysis practical. While several previous studies have focused on the analytical nature of single-particle LIBS, as noted above, the analysis of ambient air particles is also very much a statistical sampling problem. Given that LIBS typically samples a small subset of a targeted aerosol population, it is important to verify that such aliquots accurately follow the large-population statistics. Notably so, the highly dynamic nature of ambient aerosol makes the issues of temporal resolution and statistical accuracy all the more important. The current study revealed the ability of LIBS-based speciated aerosol monitoring to accurately follow in real time independently measured total aerosol counts. Of further significance, temporal resolution down to 5-minute sample intervals was found to produce accurate aerosol counts, provided sufficient sampling rates (~10 to 20 particles per sample interval) were realized. These results corroborate some of the original calculations toward discrete particle analysis in consideration of sampling limitations in view of the finite plasma volume.²³

Although excellent correlations were observed between calcium-based and sodium-based LIBS data and the light scattering based total aerosol counts, the current study also reveals the importance of full spectral coverage (e.g., simultaneous calcium and sodium analysis), and the development of more sophisticated real-time thresholding algorithms to further optimize analyte detection limits. As broadband spectral data acquisition becomes more practical (e.g., with echelle spectrometers or bundled spectrometer designs), real-time processing becomes necessary, as the collection and post-processing of enormous spectral data sets negates many of the benefits of real-time *in situ* analysis associated with LIBS. Clearly, laser-induced breakdown spectroscopy remains a promising analytical method for aerosol analysis, notably so for ambient air.

ACKNOWLEDGMENTS

This work was supported in part by the National Science Foundation through grant CTS-0317410. Any opinions, findings, and conclusions or recommendations expressed in this publication are those of the authors and do not necessarily reflect the views of the National Science Foundation.

1. G. A. Petrucci, P. B. Farnsworth, P. Cavalli, and N. Omenetto, *Aerosol Sci. Technol.* **33**, 105 (2000).
2. S. H. Wood and K. Prather, *Trends Anal. Chem.* **17**, 346 (1998).
3. D. M. Murphy and D. S. Thomson, *Aerosol Sci. Technol.* **22**, 237 (1995).
4. P. G. Carson, K. R. Neubauer, M. V. Johnston, and A. S. Wexler, *J. Aerosol Sci.* **26**, 535 (1995).
5. O. Kievit, M. Weiss, P. J. T. Verheijen, J. C. M. Marijnissen, and B. Scarlett, *Chem. Eng. Commun.* **151**, 79 (1996).
6. H. Zhang, F. Y. Yueh, and J. P. Singh, *Appl. Opt.* **38**, 1459 (1999).
7. R. E. Neuhauser, U. Panne, R. Niessner, and P. Wilbring, *Fresenius' J. Anal. Chem.* **364**, 720 (1999).
8. K. Song, Y.-I. Lee, and J. Sneddon, *Appl. Spectrosc. Rev.* **32**, 183 (1997).
9. J. Sneddon and Y.-I. Lee, *Anal. Lett.* **32**, 2143 (1999).
10. D. A. Rusak, B. C. Castle, B. W. Smith, and J. D. Winefordner, *Crit. Rev. Anal. Chem.* **27**, 257 (1997).
11. L. J. Radziemski, T. R. Loree, D. A. Cremers, and N. M. Hoffman, *Anal. Chem.* **55**, 1246 (1983).
12. D. W. Hahn, *Appl. Phys. Lett.* **72**, 2960 (1998).
13. D. W. Hahn and M. M. Lunden, *Aerosol Sci. Technol.* **33**, 30 (2000).
14. J. E. Carranza, B. T. Fisher, G. D. Yoder, and D. W. Hahn, *Spectrochim. Acta, Part B* **56**, 851 (2001).
15. G. A. Lithgow, A. L. Robinson, and S. G. Buckley, *Atmos. Environ.* **38**, 3319 (2004).
16. J. E. Carranza and D. W. Hahn, *Spectrochim. Acta, Part B* **57**, 779 (2002).
17. V. Hohreiter, J. E. Carranza, and D. W. Hahn, *Spectrochim. Acta, Part B* **59**, 327 (2004).
18. V. Hohreiter, A. Ball, and D. W. Hahn, *J. Anal. At. Spectrom.* **19**, 1289 (2004).
19. J. E. Carranza and D. W. Hahn, *Anal. Chem.* **74**, 5450 (2002).
20. J. E. Carranza, K. Iida, and D. W. Hahn, *Appl. Opt.* **42**, 6022 (2003).
21. A. McFarland, *Deposition Version 4.0*, Texas A&M University, College Station, TX (1996).
22. D. W. Hahn, J. E. Carranza, G. R. Arsenault, H. A. Johnsen, and K. R. Hencken, *Rev. Sci. Instrum.* **72**, 3706 (2001).
23. D. W. Hahn, W. L. Flower, and K. R. Hencken, *Appl. Spectrosc.* **51**, 1836 (1997).
24. C. O. Laux, R. J. Gessman, C. H. Kruger, F. Roux, F. Michaud, and S. P. Davis, *J. Quant. Spectrosc. Radiat. Trans.* **68**, 473 (2001).
25. J. E. Carranza and D. W. Hahn, *J. Anal. At. Spectrosc.* **17**, 1534 (2002).
26. S. Hoornaert, H. Van Malderen, and R. Van Grieken, *Environ. Sci. Technol.* **30**, 1515 (1996).
27. P. Laj, G. Ghermandi, R. Cecchi, V. Maggi, C. Riontino, S. M. Hong, J. P. Candelone, and C. Boutron, *J. Geophys. Res. Oceans* **102**, 26615 (1997).
28. P. B. Dixon and D. W. Hahn, *Anal. Chem.* **77**, 631 (2005).
29. N. Pomeroy, D. Webber, and C. Murphy, *Environ. Monitor. Assess.* **65**, 175 (2000).
30. S. G. Buckley, H. A. Johnson, K. R. Hencken, and D. W. Hahn, *Waste Management* **20**, 455 (2000).